A VLBI Survey of the Northern Polar Cap Region

D. D. Morabito, R. A. Preston, and J. Faulkner
Tracking Systems and Applications Section

A VLBI survey at 2.29 GHz of the northern polar cap region (declination > 69 deg) has been conducted using a baseline consisting of the NASA Deep Space Network (DSN) sites at Goldstone, California and Madrid, Spain. The purpose of this survey was to identify sources in the northern polar cap region which possess milliarcsecond components. High declination VLBI sources provide valuable geometric coverage for determining the spin axis components of baselines. Out of 48 candidate sources selected from the Bonn 5-GHz survey, 42 were detected to have compact structure on the California/Spain baseline at the 2.29-GHz observing frequency. This polar survey is part of a more general VLBI sky survey.

I. Introduction

Up to the present time, there has been an insufficient number of known high declination celestial radio sources that have strong milliarcsecond components suitable for VLBI observations. This paper presents the results of a recent search of the northern polar cap region for such VLBI sources. These results are part of a general sky survey for VLBI sources sponsored by the Deep Space Network Advanced Systems Program (Ref. 1).

High declination VLBI sources provide valuable geometric coverage for determining more accurate estimates of the spin axis components of baselines in VLBI programs aimed at clock synchronization, earth rotational orientation, and geodetic baseline measurements. The deficiency of high declination VLBI sources was due to the lack of high-frequency single antenna surveys in the northern polar cap region (declination > 69 deg). Such surveys permit sources to be identified that might possess compact structure at the milliarcsecond level.

A high-frequency single-antenna survey involving several sources from the 69- to 90-deg declination zone was recently performed at the 100-m antenna at Bonn, Germany, at 4.9 GHz (Ref. 2). Candidate high declination VLBI sources were chosen from this survey based on the following criteria:

(1) Total flux density at 4.9 GHz was greater than 0.5 Jansky.

(2) Spectral index from 2.7 to 4.9 GHz was greater than -0.6.

There were a total of 48 candidate sources selected from the Bonn survey. Of these sources, 17 had total flux densities at 4.9 GHz greater than 1 Jansky, and 31 had total flux densities between 0.5 and 1.0 Jansky. These 48 sources were then observed during three different observing sessions in March 1980.

II. Experiment Configuration

The VLBI observations were performed on March 3, 12/13, and 28, 1980, using a baseline consisting of a 26-m telescope (DSS 13) at Goldstone, California, and a 64-m telescope (DSS 63) at Madrid, Spain. The observations were performed at 2.29 GHz with right circular polarization. The receiver chain

consisted of an S-band traveling wave maser followed by a phase-stable S-band receiver (VLBI receiver at DSS 13 and BLOCK IV receiver at DSS 63) which converted the signal to an IF of 50 MHz. The Mark II (or BLOCK 0) VLBI recording system then recorded a 1.8-MHz sideband by digitally sampling at a 4-Mb/s rate. Phase stability of the receiver chain and digital sampling were controlled by hydrogen maser atomic clocks at both stations. Each observation of a source was 3 minutes in duration, with most sources being observed twice. The Goldstone-Madrid interferometer has a length of 8396 km corresponding to 64 million wavelengths at 2.29 GHz. This corresponds to a fringe spacing of 3 milliarcseconds.

III. Data Reduction

Matching tapes from both stations were then cross-correlated using the Caltech/JPL Mark II VLBI processor. Computer manipulation of the correlator output yielded the correlation coefficient for each observation or the fraction of bits on the two tapes that were correlated. The correlation coefficients were then converted into correlated flux density or the VLBI strength for each celestial radio source observation, using the procedure discussed in a previous paper (Ref. 1), with a scaling constant of 2.5 ± 0.1.

The 5-sigma detection limit for each observation was about 0.1 Jansky. Correspondingly, the uncertainty in detected source strength due to random noise was about 0.02 Jansky. However, in practice, systematic errors at about the 8% level dominate the random contribution for most sources.

The tapes must be correlated over a range of relative tape delay and delay rate offsets to compensate for a priori source position uncertainties. Appropriate searches in these parameters were performed so that the sky was completely searched within 30 arcseconds of all nominal source positions. The 6 sources not detected are assumed to have been within the range of position searching.

The measured delay and delay rate offsets for detected sources allowed the source positions to be determined to about the 0.5-arcsecond level. Instrumental biases were removed by observing sources with accurately known positions throughout each experiment. Atmospheric contributions to delay and delay rate were modeled by monthly mean values (Ref. 3) and earth rotational position was determined according to standard Bureau International de l' Heure (BIH) values of UT1-UTC and polar motion. Ionospheric effects were not modeled and are assumed to be the limiting error source. An uncertainty of 0.4 arcseconds was quadratically added to all error estimates to account for unmodeled effects. The technique of reducing the delay and delay rate observables into source positions is discussed in another paper (Ref. 4).

In addition to measurements of correlated flux density and source position, measurements of total flux density were performed at DSS 13 for most sources using a noise adding radiometer (Ref. 5). The uncertainty in the total flux density measurements is mostly due to the 0.03 kelvin errors in the measurement of system temperature, but in the case of the strong sources is dominated by the 3% errors in the value of antenna sensitivity (K/Jansky). The 0.03 K temperature uncertainty translates to a 0.3 Jansky uncertainty in total flux density. Multiple averaging of total flux density estimates results in decreased uncertainties when multiple observations are available.

Antenna sensitivity at each site was determined by using observations of flux calibration sources (Ref. 6). Pointing errors were kept to a negligible level by boresighting a few strong sources in the northern polar cap region.

IV. Results and Discussion

Of the 48 northern polar cap sources on which VLBI observations were performed, 42 were found to have detectable milliarcsecond structure. The detailed results appear in tabular form in Table 1. Notes regarding table entries appear in Table 2.

A correlated flux density histogram appears in Fig. 1. A total of three sources had correlated flux densities of greater than one Jansky, while a total of 20 sources had correlated flux densities of greater than 0.4 Jansky. A sky distribution plot of the detected 42 sources appears in Fig. 2. Here the average value of the correlated flux density was used to determine the source strength symbol used in the plot.

Since the declinations of these sources are all above 69 degrees, they are visible 24 hours a day from the antennas used in these observations. This allows a wide range of spatial frequencies to be sampled. Detectable variation in the measured correlated flux density as a function of observation time might be observable due to source structure effects. Therefore, all but six candidate sources were observed at least twice, with the observations occurring at widely different hour angles whenever possible. The following sources exhibited significant three-sigma variation in correlated flux density between observations, indicating complex structure: 0604+72, 0740+82, 4C 71.07, 0950+74, 1039+81, 1044+71, 1058+72, 3C 309.1, 1637+82, 1749+70, 1803+78, 1928+73, 1946+70, and 2007+77. Source structure may be an important consideration for high accuracy VLBI measurements, and the effects

of sources such as these on interferometric phase should be understood when selecting candidate VLBI sources.

Ten of these 48 northern polar cap sources were recently observed by Waltman et al. (Ref. 7) on a baseline having comparable resolution, but at a higher observing frequency (5 GHz).

V. Conclusion

Forty-two sources with declinations greater than 69 degrees were found to have compact structure at 2.29 GHz on the Goldstone/Madrid VLBI baseline. These northern polar sources will be useful for VLBI experiments in which determination of the spin axis components of baselines is important.

Acknowledgments

We are indebted to the instrumentation and observing assistance supplied by L. J. Skjerve of JPL, B. Johnson of Ford Aerospace and Communications Corp., F. Alcazar, B. Luaces, and D. Munoz of the Madrid Deep Space Communications Complex, and the Radio Science Support group at the Goldstone Deep Space Communications Complex. We would also like to thank the station directors at the DSN stations for supporting our program, namely, E. Jackson (DSS 13) and J. Fernandez (DSS 63).

References

1. Preston, R. A., et al., "Establishing a Celestial VLBI Reference Frame-I. Searching for VLBI Sources," *The Deep Space Network Progress Report 42-46*, May and June 1978, Jet Propulsion Laboratory, Pasadena, Calif., Aug. 15, 1978.

2. Kuhr, H., Nauber, V., Pauliny-Toth, I. I. R., Witzel, A., "A Catalogue of Radio Sources", Max-Planck-Institut fur Radioastronomie, Preprint No. 55, August 1979.

3. Thuleen, K. L., and Ondrasik, V. J., "The Repetition of Seasonal Variations in the Tropospheric Zenith Range Effect," in *The Deep Space Network Progress Report*, Technical Report 32-1526, Vol. VI, pp. 83-98, Jet Propulsion Laboratory, Pasadena, Calif., Dec. 15, 1971.

4. Morabito, D. D., et al., "Arcsecond Positions for Milliarcsecond VLBI Nucleii of Extragalactic Radio Sources; Part I: 546 Sources," to be published in the *Astronomical Journal*, 1981.

5. Reid, M. S., Gardner, R. A., and Stelzried, C. T., "A New Broadband Square Law Detector," JPL Technical Report 32-1599, Jet Propulsion Laboratory, Pasadena, Calif., Sept. 1, 1975.

6. Klein, M. J., and Stelzried, C. T., "Calibration Radio Sources for Radio Astronomy: Precision Flux-Density Measurements at 2295 MHz," *The Astronomical Journal*, Vol. 81, 1078, 1976.

7. Waltman, E., et al., "Compact Radio Sources at Declinations Greater Than 67 Degrees," submitted to *Astronomy and Astrophysics*, 1981.

8. Fanselow, J. L., private communication.

Table 1. Northern polar survey results

(1) SOURCE NAME	(2) RIGHT ASCENSION HR	MIN	SEC	ERROR	(3) DECLINATION DEG	MIN	SEC	ERROR	(4) REF CODE	(5) EXPERIMENT	(6) TOTAL FLUX DENSITY (JY)	+/-	(7) CORRELATED FLUX DENSITY (JY)	+/-	(8) VISIBILITY	+/-	(9) SPATIAL FREQUENCIES U	V
0014+81	0	14	4.472	0.026	+81	18	28.72	0.28		B	1.0	0.3	0.34	0.03	0.3	0.1	-40.6	49.5
										C			0.35	0.03	0.4	0.1	-57.9	27.5
0016+73	0	16	54.200	0.022	+73	10	51.41	0.06	1	B	1.5	0.1	0.50	0.04	0.33	0.03	-42.9	46.6
										C			0.54	0.04	0.36	0.04	-49.2	40.3
0018+72	0	18	34.483	0.034	+72	56	3.93	0.30		B	0.8	0.2	0.11	0.01	0.14	0.04	-43.7	45.8
										C			0.11	0.01	0.14	0.04	-50.0	39.3
0027+70	0	27	17.026	0.033	+70	21	6.26	0.41		C	0.8	0.1	0.21	0.02	0.26	0.04	-49.8	39.1
0149+71	1	49	20.814	0.022	+71	0	20.76	0.30		B	1.5	0.2	0.18	0.02	0.12	0.02	-27.7	55.8
										C			0.16	0.01	0.11	0.02	-34.1	52.4
0153+74	1	53	4.339	0.019	+74	28	5.69	0.28		B	2.1	0.2	0.66	0.05	0.31	0.04	-28.3	56.3
										C			0.71	0.06	0.34	0.04	-34.5	52.9
0205+72	2	5	26.907	0.019	+72	15	16.40	0.28		B	0.8	0.2	0.41	0.03	0.5	0.1	-28.6	55.7
										C			0.38	0.03	0.5	0.1	-35.2	52.1
0212+73	2	12	49.935	0.019	+73	35	40.15	0.28		B	2.3	0.2	1.04	0.08	0.45	0.05	-28.6	56.0
										C			1.01	0.08	0.44	0.05	-34.8	52.6
0403+76	4	3	59.196	0.019	+76	48	52.75	0.31		B	4.4	0.1	0.11	0.01	0.025	0.002	-4.9	63.0
										C			0.14	0.01	0.032	0.002	-9.7	62.4
0454+84	4	54	57.213	0.019	+84	27	53.02	0.28		B	1.3	0.1	0.90	0.07	0.69	0.08	8.5	63.5
										C			0.80	0.06	0.62	0.07	4.2	63.9
0604+72	6	4	39.237	0.020	+72	49	27.21	0.29		B	1.0	0.2	0.19	0.02	0.19	0.04	20.2	59.1
										C			0.28	0.02	0.28	0.06	14.2	60.7
0615+82	6	15	32.80		+82	03	56.5		3	B	1.3	0.3	0.61	0.05	0.5	0.1	21.9	60.1
										C			0.64	0.05	0.5	0.1	20.0	60.7
0633+73	6	33	6.438	0.027	+73	27	35.75	0.41		C	0.9	0.3	0.36	0.03	0.4	0.1	20.2	59.2
0716+71	7	16	13.061	0.022	+71	26	14.92	0.41	1	B	0.7	0.3	0.11	0.01	0.16	0.07	31.8	53.8
										C			0.11	0.01	0.16	0.07	29.3	55.1
0718+79	7	18	8.892	0.019	+79	17	22.60	0.28		B	1.0	0.2	0.51	0.04	0.5	0.1	23.6	59.1
										C			0.50	0.04	0.5	0.1	28.2	57.2
0740+82	7	40	33.222	0.027	+82	49	24.17	0.29		A	1.6	0.3	0.42	0.04	0.26	0.06	60.4	21.5
										C			0.27	0.02	0.17	0.03	32.5	55.2
4C 71.07	8	36	21.558	0.009	+71	4	22.46	0.03	2	A	4.4	0.3	0.63	0.05	0.14	0.01	62.6	13.8
										A			0.37	0.03	0.084	0.009	13.3	60.3
0950+74	9	50	4.573	0.032	+74	50	7.67	0.29		A	1.2	0.3	0.19	0.02	0.16	0.04	63.8	-3.8
										A			0.12	0.01	0.10	0.03	54.2	33.8
1003+83	10	03	25.911	0.041	+83	04	56.52	0.40		A	1.1	0.3	0.43	0.04	0.4	0.1	63.1	11.5
1011+81	10	11	52.2		+81	20	16.		3	A	0.6	0.3	<0.05		<0.08		63.1	11.4
										C			<0.05		<0.08		45.8	44.8
1039+81	10	39	27.821	0.024	+81	10	23.54	0.28		A			0.38	0.03			63.8	5.8
										C			0.63	0.05			48.8	41.5
1044+71	10	44	49.741	0.019	+71	59	26.73	0.28		A	1.0	0.2	0.73	0.06	0.7	0.2	63.8	-4.3
										C			0.95	0.08	1.0	0.2	56.0	30.6
1049+72	10	49	06.8		+72	15	42.		3	A	0.8	0.2	<0.04		<0.05		62.6	-11.7
										C			<0.05		<0.06		58.1	26.7
1053+70	10	53	27.730	0.020	+70	27	47.78	0.28		A	0.6	0.3	0.59	0.05	1.0	0.5	62.0	-14.0
										C			0.66	0.05	1.1	0.6	59.4	23.7
1053+81	10	53	36.302	0.019	+81	30	35.41	0.23		A	0.6	0.3	0.42	0.04	0.7	0.4	63.9	3.9
										B			0.51	0.04	0.8	0.3	60.2	22.2
										C			0.50	0.04	0.8	0.4	51.0	38.8
1058+72	10	58	20.116	0.022	+72	41	44.72	0.28		A	1.0	0.2	0.56	0.05	0.6	0.1	63.6	-6.1
										C			0.21	0.02	0.21	0.05	56.7	29.4
1150+81	11	50	23.48		+81	15	10.2		3	A	1.2	0.3	0.76	0.07	0.6	0.2	63.2	-9.4
										C			0.88	0.07	0.7	0.2	58.0	27.4
1221+80	12	21	47.662	0.036	+80	56	41.03	0.28		A			0.18	0.02			61.9	-15.8
										C			0.21	0.02			60.5	21.4

Table 1 (contd)

(1) SOURCE NAME	(2) RIGHT ASCENSION HR	MIN	SEC	ERROR	(3) DECLINATION DEG	MIN	SEC	ERROR	(4) REF CODE	(5) EXPERI-MENT	(6) TOTAL FLUX DENSITY (JY)	+/-	(7) CORRELATED FLUX DENSITY (JY)	+/-	(8) VISIBILITY	+/-	(9) SPATIAL FREQUENCIES U	V
1305+80	13	5	22.146	0.034	+80	24	21.27	0.24		A	0.7	0.3	0.15	0.02	0.21	0.10	58.5	-25.0
										B			0.13	0.01	0.19	0.08	-25.3	-57.4
										C			0.14	0.01	0.20	0.09	62.9	12.2
1345+73	13	45	14.2		+73	35	46.		3	A	1.0	0.3	<0.04		<0.04		60.0	-20.6
										B			<0.05		<0.05		-24.1	-55.9
1357+76	13	57	42.177	0.035	+76	57	53.05	0.40		A			0.26	0.02			52.2	-35.3
1436+76	14	36	4.574	0.077	+76	18	23.82	0.45		A	1.3	0.3	0.07	0.01	0.05	0.01	51.4	-36.2
1448+76	14	48	56.496	0.022	+76	13	33.81	0.28		A	1.0	0.3	0.44	0.04	0.4	0.1	50.4	-37.5
										B			0.37	0.03	0.4	0.1	-40.2	-47.6
3C 309.1	14	58	56.646	0.015	+71	52	11.15	0.06	2	A			0.14	0.01			50.9	-35.8
										A			0.08	0.01			63.9	5.1
										B			0.53	0.05			-39.0	-47.2
										B			0.14	0.01			-4.3	-59.6
1557+70	15	57	37.1		+70	49	45.		3	A	1.4	0.3	<0.05		<0.04		41.3	-45.1
										B			<0.05		<0.04		-49.4	-37.4
1612+79	16	12	21.8		+79	47	30.		3	A	1.3	0.3	<0.04		<0.03		39.9	-48.6
										B			<0.05		<0.04		-50.4	-38.2
1616+85	16	16	22.349	0.256	+85	9	26.04	0.49		A	1.1	0.3	<0.05		<0.04		48.3	-41.6
										B			0.07	0.01	0.06	0.02	-48.1	-41.9
1637+82	16	37	56.849	0.045	+82	38	18.48	0.30		A	2.1	0.3	0.12	0.01	0.057	0.009	42.2	-47.3
										B			0.24	0.02	0.11	0.02	-52.7	-35.7
1749+70	17	49	03.399	0.021	+70	06	39.44	0.25	1	A	1.1	0.3	0.22	0.02	0.20	0.06	28.4	-52.8
										B			0.34	0.03	0.31	0.09	-59.4	-21.4
1803+78	18	03	39.207	0.038	+78	27	54.08	0.23	1	B	2.6	0.2	0.75	0.06	0.29	0.03	-59.2	-23.2
										B			1.53	0.12	0.59	0.06	6.5	-61.7
1807+69	18	7	18.503	0.020	+69	48	57.07	0.28		B	3.1	0.3	1.01	0.08	0.33	0.04	7.2	-58.5
1825+74	18	25	56.1		+74	19	05.		3	A	1.0	0.3	<0.05		<0.05		27.6	-54.7
										B			<0.05		<0.05		-60.7	-18.6
1928+73	19	28	49.333	0.040	+73	51	44.67	0.20	1	A	3.0	0.3	0.45	0.04	0.15	0.02	13.0	-59.3
										B			0.77	0.06	0.26	0.03	-63.9	-3.7
1946+70	19	46	12.034	0.028	+70	48	21.66	0.32		A	0.7	0.3	0.17	0.02	0.2	0.1	10.2	-58.6
										B			0.06	0.01	0.09	0.04	-64.0	-.3
2007+77	20	07	20.478	0.060	+77	43	58.12	0.18	1	A	1.2	0.3	1.09	0.09	0.9	0.2	8.3	-61.3
										B			0.68	0.05	0.6	0.1	-64.0	.5
2010+72	20	10	16.193	0.020	+72	20	20.81	0.28		A	1.5	0.3	0.59	0.05	0.39	0.09	5.1	-59.8
										B			0.53	0.04	0.35	0.08	-64.0	3.9
2136+82	21	36	2.188	0.029	+82	25	38.61	0.30		A	1.1	0.3	0.17	0.02	0.15	0.05	-10.7	-62.2
										B			0.12	0.01	0.11	0.03	-61.4	18.6
2229+69	22	29	11.643	0.019	+69	31	2.79	0.29		A			0.43	0.04			-23.3	-54.7
										B			0.54	0.04			-56.1	30.1

Table 2. Notes for Table 1

Column	Description
1	Source name
2,3	Source position: right ascension and declination. The positions are referenced to the equinox of 1950.0, and elliptical aberration terms are included so as to agree with past astronomical convention.
4	Source position reference code: If no reference code is given, the position was estimated from the delay and delay rate observables. Otherwise the position was obtained from one of the following references:

Code	Reference
1	Waltman et al. (Ref. 7)
2	JPL Reference Frame Catalog (Ref. 8)
3	Bonn Catalog (Ref. 2)

The detected sources whose positions came from these references had well-known positions and allowed instrumental biases to be calibrated.

5	Experiment codes: A = 3 March 1980 B = 12/13 March 1980 C = 28 March 1980
6	Total flux density and uncertainty in Jy.
7	Correlated flux density and uncertainty in Jy.
8	Fringe visibility and uncertainty: Defined as the ratio of correlated flux density to total flux density or the fraction of flux density detected by the interferometer as coming from the milliarcsecond core.
9	Spatial frequencies: U is the east-west component of the baseline projection against the sky, and V is the north-south component of the baseline projection against the sky. These are given in millions of wavelengths.

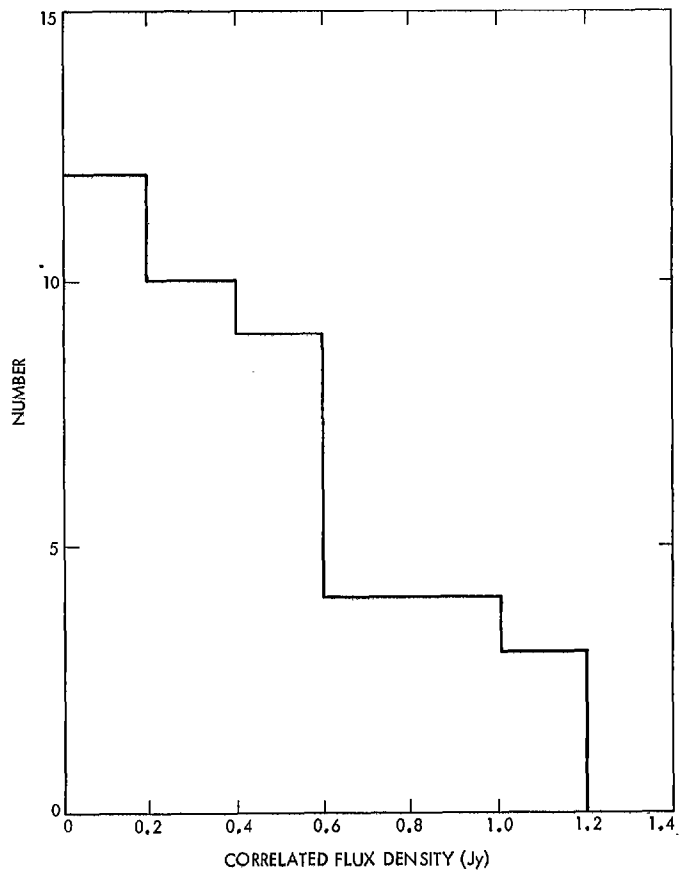

Fig. 1. Correlated flux density histogram

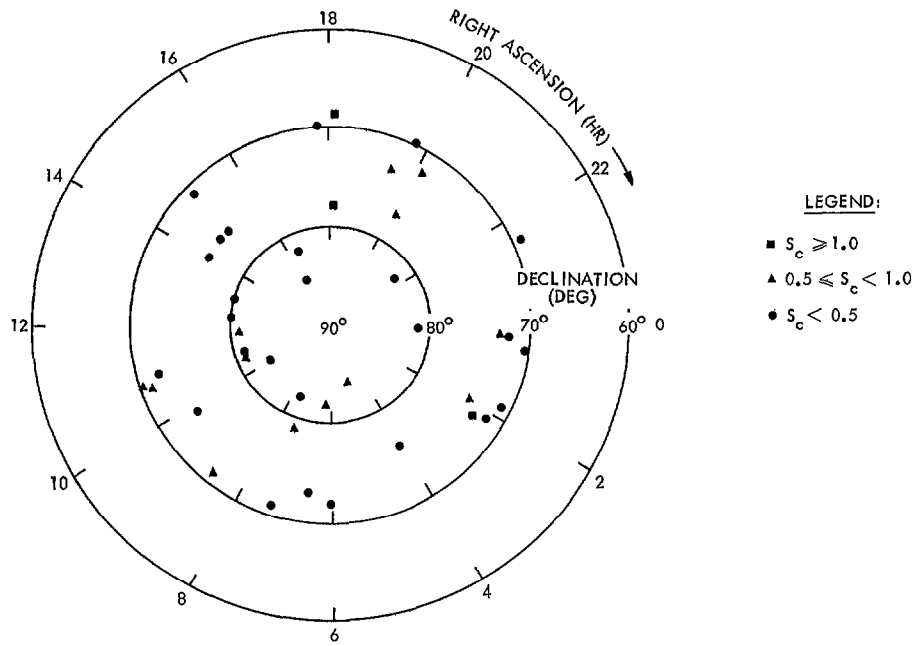

Fig. 2. Sky distribution plot of detected sources